Arch Appl Mech (2013) 83:509–519
DOI 10.1007/s00419-012-0700-y

ORIGINAL

Krzysztof Mendrok · Piotr Kurowski

Operational modal filter and its applications

Received: 4 January 2012 / Accepted: 22 August 2012 / Published online: 7 September 2012

Abstract In the paper, the procedure for the estimation of modal filter coefficients from output-only data is presented. The basic concept of the procedure consists in frequency response functions synthesis based on the knowledge of an operational modal model. A method of operational mode shapes scaling is described. The method is then compared with the classical modal filter and with modal filtration of responses spectra, which is sometimes used as a solution for modal filtration based on the output-only data. Each solution is applied to load identification and damage detection. The study shows the method verification on data obtained from laboratory experiment.

Keywords Modal filtration · Operational modal analysis · Damage detection · Load identification

1 Introduction

In recent years, several teams of researchers have developed the use of modal filters and have applied the results of such analyses in the tasks of vibration control, damage detection, and load identification [1–13]. Generally speaking, the modal filter extracts the modal coordinates of each individual mode from a system's output. This is achieved by mapping the response vector from the physical space—the network of measurement points to the modal space. It was first introduced by Baruh and Meirovitch in 1982 [14] with the aim of overcoming the spillover problem encountered while controlling distributed parameter systems. They used representation of the modal filter for the distributed parameter system, which had a following drawbacks: necessity to know the function of the spatial distribution of mass (which is possible only for simple geometries) and the vibration response measurement performed at each point of the object. To avoid this second problem, the authors proposed a method using interpolated function of measurements from sensors located in a finite number of points. Then, the filtration accuracy, however, depends on the quality of interpolation. Therefore, in early 90s of the previous century, the discrete modal filter was formulated [15,16]. Since then, the modal filter has been applied to: active vibration reduction, the correlation of experimental modal models with theoretical models obtained by finite element method (FEM), the identification of operational forces, and finally to damage detection. These latter groups of applications are the main interest of the authors. Modal filtration in the field of damage detection has many advantages including its autonomous operation (without the interaction of qualified staff), low computational cost, and low sensitivity to changes in external conditions [5]. However, the main drawback of this group of damage detection methods is its limited applicability to operational data. In the literature,

K. Mendrok (✉) · P. Kurowski
Department of Robotics and Mechatronics, AGH University of Science and Technology,
al. A. Mickiewicza 30, 30-059 Kraków, Poland
E-mail: mendrok@agh.edu.pl

P. Kurowski
E-mail: kurowski@agh.edu.pl

the modal filtration of the responses power spectral densities (PSDs) [instead of frequency response functions (FRFs)] has been proposed [4]. However, this approach frequently does not provide the desired results, as it only works properly for excitations in the form of white noise or an ideal impulse. In this paper, a different approach is described. The basis for it are FRFs synthesized using knowledge of the operational modal model. A method of operational mode shape scaling is also described. This is based on the measurements of several FRFs of the object. Such an approach is much more complex and less computationally efficient but it has the advantage that its results are proper for any kind of excitation signal.

2 Modal filter theory

As it was stated in the previous section, the discrete modal filter theory can be found in [15,16]. In this section, only the calculation of reciprocal modal vectors according to Mendrok and Uhl [5] is reminded. The construction of the rth discrete modal filter, which corresponds to the rth pole of the transfer function $H(\omega)$, is based on the assumption that the modal residue R_{rpp} is in the imaginary form [5]:

$$R_{rpp} = j \cdot 1 \tag{1}$$

Next, the 1 DOF FRF $H_{pp}(\omega)$ is determined:

$$H_{pp}(\omega) = \frac{R_{rpp}}{j\omega + \lambda_r} + \frac{R^*_{rpp}}{j\omega + \lambda^*_r} \tag{2}$$

where λ_r—the rth pole of the system.

For the given frequency range, the above FRF is determined in the k values:

$$H_{pp}(\omega) = [H_{pp}(\omega_1)\, H_{pp}(\omega_2)\, \ldots\, H_{pp}(\omega_k)]^T \tag{3}$$

With the assumption that a single excitation was used and the response signals were measured in N points, the experimental FRFs matrix can be presented as the $k \times N$ matrix:

$$H_{kN}(\omega) = \begin{bmatrix} H_1(\omega_1) & H_2(\omega_1) & H_N(\omega_1) \\ H_1(\omega_2) & H_2(\omega_2) & H_N(\omega_2) \\ & \vdots & \\ H_1(\omega_k) & H_2(\omega_k) & H_N(\omega_k) \end{bmatrix} \tag{4}$$

The FRF matrix formed in this way is used for the determination of the reciprocal modal vectors matrix Ψ:

$$\Psi = H^+_{kN} \cdot H_{pp} \tag{5}$$

where $^+$—denotes a pseudo-inverse of the matrix.

The reciprocal modal vectors should be orthogonal with respect to the modal vectors, and thanks to this condition, they can be applied to the decomposition of the system responses to modal coordinates η_r.

$$\eta_r(\omega) = \Psi_r^T \cdot \{x(\omega)\} = \left(\frac{\{\phi_r\}^T}{j\omega - \lambda_r} + \{\psi_r\}^T \{\phi^*_r\} \frac{\{\phi^*_r\}^T}{j\omega - \lambda^*_r} \right) \{f(\omega)\} \tag{6}$$

where ϕ_r—the rth modal vector, $\{x(\omega)\}$—vector of system responses, $\{f(\omega)\}$—vector of excitation force.

3 FRFs synthesis using scaled operational modal model

Scaling operational mode shapes can be performed in several different ways. The general assumption is that it is necessary to acquire additional knowledge concerning the tested object. This knowledge can be gained through the use of:

- an analytical model of the tested object, e.g. the finite element model,
- methods for investigating the sensitivity of modal parameters to the known changes in the parameters of the tested structure,

– additional measurement characteristics collected during testing,
– cepstral analysis.

Using the first group of methods appears to be quite obvious. The idea behind the use of the analytical model parameters (e.g., mass or stiffness matrix) for the tested object seems to be fairly simple. The difficulty is, however, to create a suitably tuned analytical model describing the dynamics of the tested object. Necessary knowledge related to the parameters of material resources and detailed geometric modeling are often too limited for the application of this method. The successful application of this kind of scale in the study of bridge constructions is shown in [17]. The techniques used in this example have enabled the use of FEM for the scaling of operational mode shape.

The second group of methods based on the study of the sensitivity of modal parameters to controlled changes to the tested object are the most frequently used. In most cases, a modified parameter of the object is a matrix of the masses. The change is mostly at one [18,19] or more [20] measurement points. The techniques used to determine the scaling coefficients are based on different assumptions. The most important of the assumptions adopted for each of the methods discussed in this group is the need to at least double the implementation of the modal experiment. The first test is performed on the unmodified object and the second after the introduction or removal of a known mass or set of the masses. Both experiments are performed on the same network points and assume similar operating conditions to force the object. In the simplest case [18–22], it is assumed that a slight modification of the mass at a point disturbs only the natural frequencies and does not change the mode shape. The formulation according to scaling in this case can be performed independently for each identified mode shape. Another concept was concluded in [23]. In this case, it is assumed that the mass modification can affect both the pole change of the object and also be reflected in the local shape modification. In this case, the issue of estimating scaling factors, however, requires a global approach and the designation of all the factors in a single optimization.

The third group of methods is the least discussed in the literature. This approach assumes the estimation of scaling factors based on an additionally performed set of transfer function characteristics measurements. This method was first successfully applied to determine the scaling coefficients of the model obtained on the basis of the acoustic excitation [24,25]. Its idea is based on the operational measurement of the points in the defined network. In addition to the selected point network, it is necessary to measure the point characteristics using pulsed excitation (with measured excitation force). On the basis of the operational modal model parameters, the point characteristics are reconstructed at the points where the measured point characteristics were known. Realization of a comparison of characteristics allows the estimation of missing scaling factors.

The fourth group consists of the methods proposed in [26,27]. These works were conducted by a team led by Prof. B. Randall. The method involves the reconstruction of the frequency response function using cepstrum analysis. The method allows the reconstruction of FRF force structure functions, assuming a single impulse of force at a given location. In [27], the method is extended by the additional possibility of a broadband noise signal in addition to the excitation.

The presented methods show that the issue of scaling can be solved in at least a couple of ways. Taking into account the fact that the creation of the updated FEM models is very difficult, the first group of methods appears to be of limited use for the case of operational measurements. A similar impression applies to the methods of cepstral analysis. Very complex mathematical apparatus associated with the intensive use of nonlinear optimization methods makes these methods less relevant to the determination of a scaling factor-derived modal model based on operational measurements. Accordingly, for further analysis, methods based on the sensitivity of modal parameters to changes in the parameters of the mass of the tested structures, and methods to estimate the scaling factors based on the additional measurements of the transfer characteristics in the selected measurement points network, were selected.

3.1 Determination of scaling for measurement of additional characteristics

In the case of the use of additional measurement characteristics for scaling the estimated mode shape, we assume the existence of modal model parameters in advance. These parameters are:

λ_r—system poles obtained on the basis of operational data
ϕ_r—unscaled mode shapes obtained on the basis of operational data.

The formulation of a classical modal model is often described by the equation, which is represented in the frequency domain [28], as follows:

$$H(\omega) = \sum_{r=1}^{N} \left(\frac{Q_r \Psi_r \Psi_r^t}{j\omega - \lambda_r} + \frac{Q_r^* \Psi_r^* \Psi_r^* t}{j\omega - \lambda_r^*} \right) \tag{7}$$

where $H(\omega)$—spectral transfer function matrix, Ψ_r—mode shapes vector corresponding to the pole r, Q_r—scaling factor of the rth mode shape, λ_r—rth system pole, N—number of system poles.

Assuming $\overline{Q_r}\varphi_{pr}\varphi_{qr} = Q_r \Psi_{pr} \Psi_{qr}$ we obtain:

$$H_{pq}(\omega) = \sum_{r=1}^{N} \frac{\overline{Q_r}\varphi_{pr}\varphi_{qr}}{j\omega - \lambda_r} + \frac{\overline{Q_r^*}\varphi_{pr}^*\varphi_{qr}^*}{j\omega - \lambda_r^*} \tag{8}$$

Scaling coefficients can be determined by the least squares formulation of the task. Estimation of the scale factor can be improved by choosing a set of points on the tested structure and the appointment of several transfer characteristics at these points.

The method assumes that the operating model and the one built-in classical circumstances converge. In the case of nonlinear objects, it may be possible that differences in the operational and classical modal model are large enough to prevent it from obtaining the correct scaling factors.

In the case of determining the scaling factor for operational mode shapes, the additional measurement of the transient measurements at only a few points on the tested structure is required, which significantly simplifies the implementation of the experiment. In the case of other methods, such as use of the additional mass, scaling is necessary to repeat the whole measurement process at all points of the assumed measurement network. Knowledge of additional transfer characteristics is required at a minimum of one pair of points. In this case, the designation of a scaling algorithm is as follows:

- operational performance of the modal test in a defined network of measurement points,
- additional measurement of the transient behavior for at least one pair of points contained in the previously established network of measurement points,
- performance of the modal parameter estimation model for the operational data set,
- based on estimated modal parameters of the model and additional collected transfer characteristics, formulation of the least-squares problem,
- solution to the problem of least squares, providing the sought scaling coefficients.

4 Verification of the method on the experimental data

The laboratory stand used for experimental validation of the proposed procedure consists of a steel frame excited with an electrodynamic shaker. Vibrations were measured by accelerometers placed on the frame. A photo of the test setup without sensors and measuring equipment is presented in Fig. 1, and the network of measuring points is presented in Fig. 2.

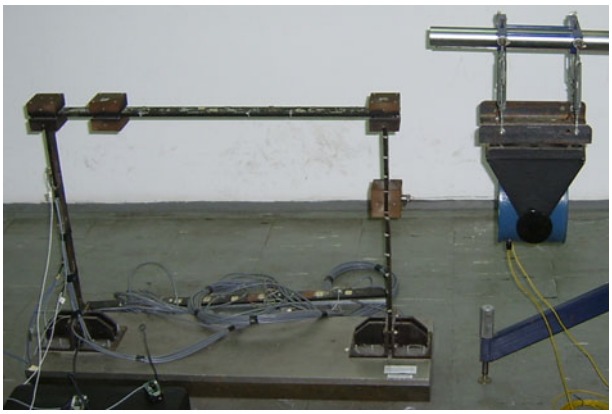

Fig. 1 The test object

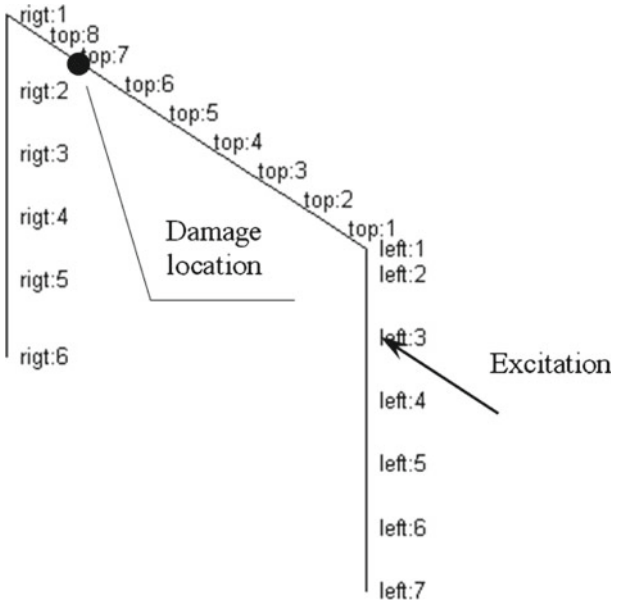

Fig. 2 Measuring points net

Table 1 Modal parameters of the laboratory stand

MS no.	EMA		OMA	
	N. f. (Hz)	Modal d. c. (%)	N. f. (Hz)	Modal d. c. (%)
1	10.82	7.01	11.03	3.35
2	43.63	1.53	43.34	1.29
3	54.52	1.99	60.39	2.49
4	120.74	1	119.49	0.75
5	61.7	0.7	159.69	0.49
6	227.73	1.23	228.91	1.23

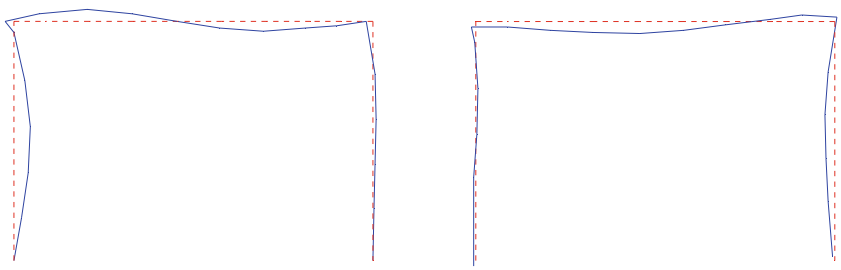

Fig. 3 Comparison of estimated mode shape no. 3 with use of EMA (*left-hand side*) and OMA (*right-hand side*)

In the course of experiment, time histories of the excitation force and accelerations of vibrations at each measuring point were recorded. As was established in the procedure, the data from the test were used to estimate both FRFs and cross-spectral densities. Both experimental and operational modal analyses were carried out. Table 1 presents the obtained modal parameters.

Comparing the results of modal model estimation in case of classical and operational approach, it can be concluded that in the case of the five poles, the values are in the range of measurement and estimation errors. The third pole obtained for both the classical and operational case is relatively poorly mapped in measured data. An analysis of estimation results can be inferred that these are probably two different poles of the subject estimated in such a way that one of them is detected by operational modal analysis algorithms and the other by classical analysis algorithm. In Fig. 3, comparison of mode shape no. 3 obtained in both analyses is placed.

The presented comparison showed that these two modes are different. This proves that the third pole identified with the use of EMA is not the same pole that was identified with the use of OMA.

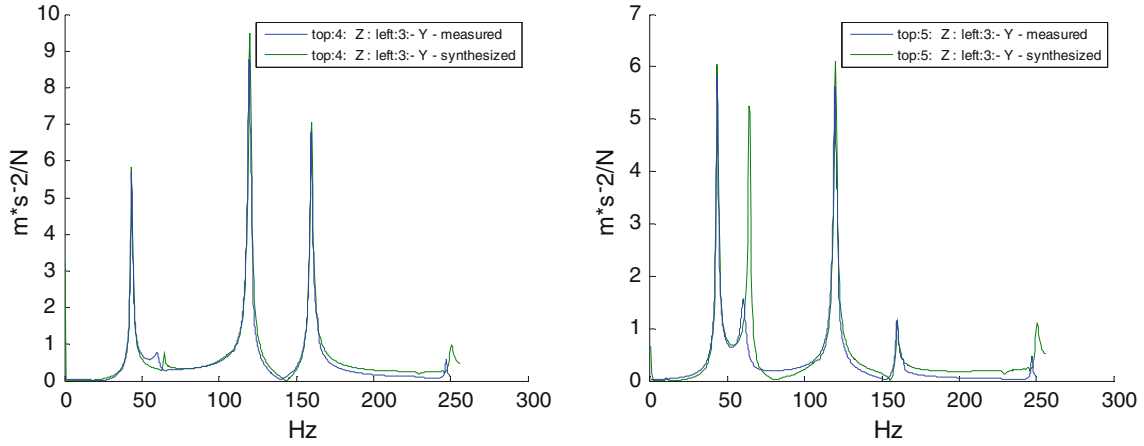

Fig. 4 Comparison of measured and synthesized FRFs

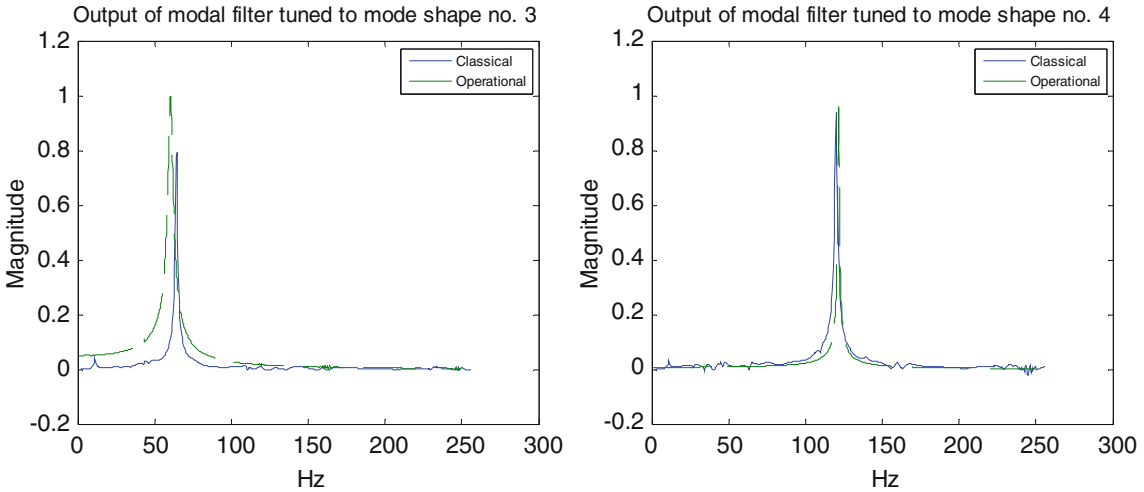

Fig. 5 Comparison of modal filtration with the use of classical and operational approaches

4.1 Comparison of classical and operational modal filter

Next, three of the measured FRFs were used for operational modal model scaling. Scaled modal model was next used for FRFs synthesis, and these FRFs were used for modal filter coefficients estimation. The results of such an operational modal filtration were compared with classical modal filtering. In Fig. 4, comparison between FRFs measured and synthesized with the use of the described procedure is placed.

As is visible from the examples in Fig. 4, the convergence between the measured and synthesized FRFs is acceptable except in the region of third natural frequency. The reason for that was explained in the previous section. The authors decided not to repeat the test, while such a situation could happen during measurements for damage detection purposes and the method should be robust for such phenomena. Additionally, the modes 1 and 6 are not evident on the presented FRFs due to the fact that they correspond to the structure motion in perpendicular direction (X—according to the experiment notation). In Fig. 5, the results of modal filtration with the use of a classical modal filter and with the use of an operational modal filter are compared.

As is visible from the presented examples, the synthesized FRFs from a scaled operational modal model can be easily applied for modal filtration. Obtained results are almost identical to the ones from a classical modal filter. There are, of course, some differences in mode shape no. 3, but they do not disqualify the method, since the reason for that is in the measurements.

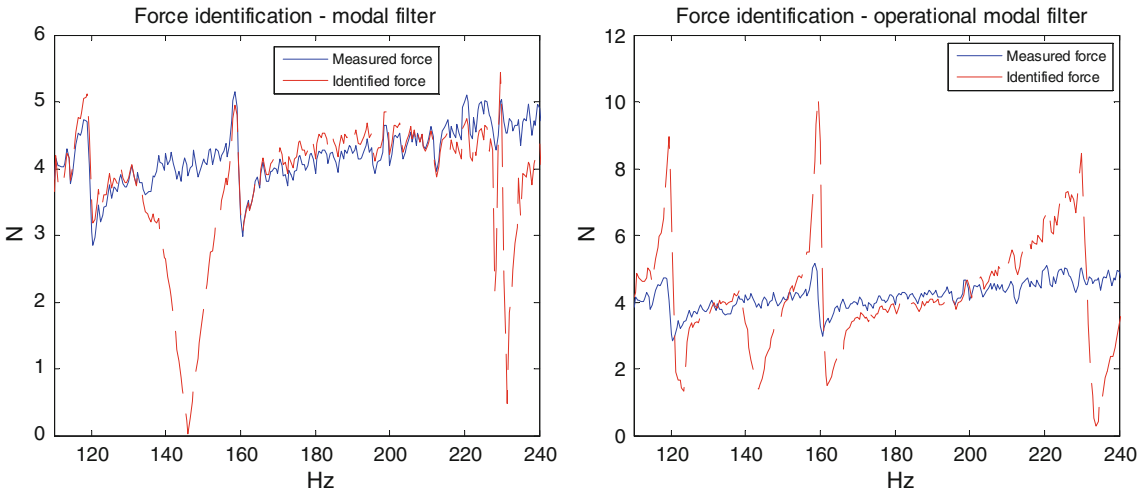

Fig. 6 Comparison of force identification with the use of classical and operational approaches

4.2 Results of identification of excitation force

In the next step, both classical and operational modal filters were used to excitation force identification. The same laboratory data were used for that purpose. The excitation force in form of pass band noise was measured during the experiment and next applied for comparison with the identified one. The force identification algorithm based on the modal filter was developed by Shih et al. in 1989 [29], and it proceeds in four major steps:

1. Transfer the outputs of the system from physical coordinates to modal coordinates using modal filters.
2. Determine the number of uncorrelated system inputs based on the weighted modal coordinates.
3. Locate these unknown inputs.
4. Calculate the amplitude of these inputs.

The last steps of the procedure are executed by the following equations:

$$\frac{\hat{\eta}_r(\omega)}{\lambda_r^* - \lambda_r} = \{\phi_r\}^T \{f(\omega)\} \tag{9}$$

where $\hat{\eta}_r(\omega) = \eta_r(\omega)(j\omega - \lambda_r)(j\omega - \lambda_r^*)$

Or, in matrix form:

$$[F] = [\Phi]^{T+}[\Pi] \tag{10}$$

where:

$$[\Pi] = \begin{bmatrix} \frac{\hat{\eta}_1(\omega_A)}{\lambda_1^* - \lambda_1} & \cdots & \frac{\hat{\eta}_1(\omega_Z)}{\lambda_1^* - \lambda_1} \\ \vdots & \ddots & \vdots \\ \frac{\hat{\eta}_n(\omega_A)}{\lambda_n^* - \lambda_n} & \cdots & \frac{\hat{\eta}_n(\omega_Z)}{\lambda_n^* - \lambda_n} \end{bmatrix}$$

$$[F] = [f(\omega_A) \cdots f(\omega_Z)] \tag{11}$$

Note that the dimension of the input vector $f(\omega)$ is defined to be the same as that of the modal vector. This is why many of its rows must be zero, except those corresponding to the vibration sources, that is, the rank of the matrix $[F]$ equals the number of uncorrelated input forces. Since $[\Phi]$ is a full rank matrix, the rank of $[\Pi]$, which contains the weighted modal coordinates should be the same as the rank of $[F]$. As a result, the number of vibration sources can be determined by inspecting the singular values of the matrix $[\Pi]$.

Using above procedure, the excitation force was calculated from the same output data. The results of calculations are presented in Fig. 6.

Table 2 Comparison of results of force identification

Criterion of comparison	Modal filter	Operational modal filter	Measured force
Correlation coefficient	0.725	0.776	1
RMS value	4.04	4.25	4.72

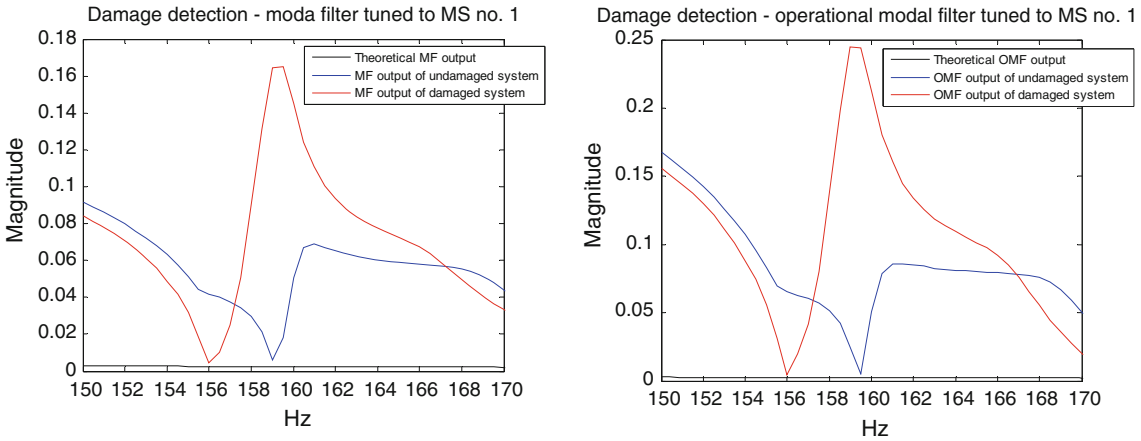

Fig. 7 Comparison of damage detection with the use of classical and operational approaches

The visual assessment of the results of identification shows that in both cases, there are problems with identification accuracy in area of resonances and anti-resonances. The reason for that is partially in the fact that authors did not use any regularization algorithm. These problems seem to be much less in case of classical modal filter. On the other hand, identification quality criteria selected by the authors give a little advantage to the operational modal filter. These criteria were correlation coefficient calculated between measured and identified force spectra and their RMS value. In Table 2, results of force identification are presented.

This application of modal filtration showed that operational modal filter is capable of identifying force with accuracy comparable to the classical solution. It is, however, important to mention that the identification errors in characteristic frequencies are lower for the classical modal filter.

4.3 Results of damage detection

In the consecutive step, the tested frame was nicked in the measuring point top:7. The depth of the cut amounted 5 mm (12.5 % of the cross-section reduction). With the same configuration of the measuring equipment, the modal test was repeated. During this test, the time histories of the excitation force and responses accelerations were measured. This time data were then used to calculate the FRFs and PSDs.

There are several methods of modal filter application to damage detection [1–5]. The authors used the one described in [5]. It is based on the fact that the FRF of an object filtered with a modal filter has only one peak corresponding to the natural frequency to which the filter is tuned. When a local change occurs in the object—in stiffness or in mass (this mainly happens when damage in the object arises)—the filter stops working and, on the output characteristic, other peaks start to appear, corresponding to other imperfectly filtered natural frequencies. To test the ability of the operational modal filter to damage detection and compare it with classical modal filter and modal filtration of PSDs, three damage detection procedure were carried out:

1. filtration of the “damaged” FRFs with use of classical modal filter,
2. filtration of the “damaged” PSDs with use of classical modal filter,
3. filtration of the “damaged” synthesized FRFs with use of operational modal filter.

Results of comparison of first two procedures is presented in Fig. 7.

In the figure on both plots, the area of natural frequency no. 5 is enlarged. It is quite clear that both approaches work similarly. The worsening of filtration effect is visible. To compare both filters in more quantitative way, the damage index was calculated. The index is calculated as a relative difference between reference and “damaged” characteristics modally filtrated with the use of the following formula:

Table 3 Comparison of results of damage detection

	Modal filter	Operational modal filter
Damage index for consecutive mode shapes	0.067	0.055
	0.091	0.024
	0.074	0.034
	0.016	0.034
	0.008	0.014
	0.108	0.126

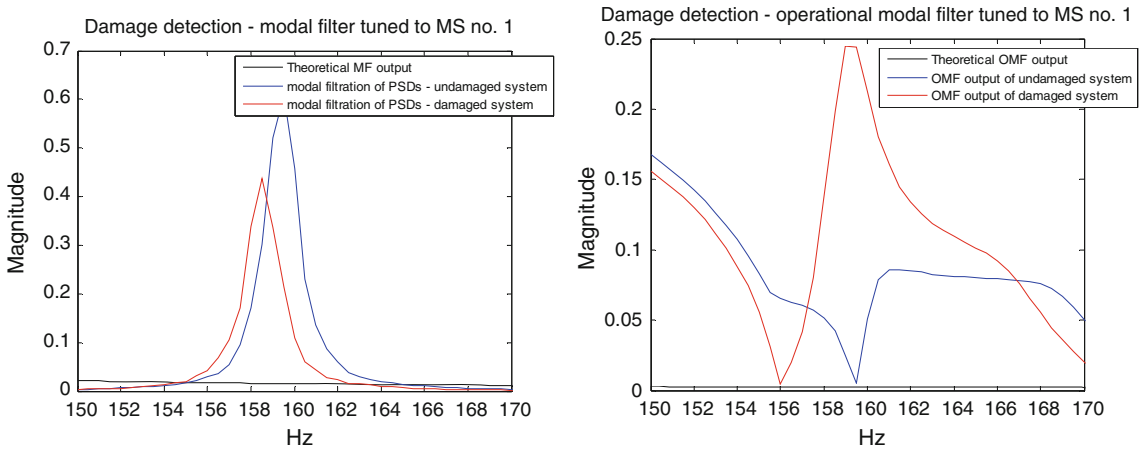

Fig. 8 Comparison of damage detection with the use of classical modal filtration of responses signals and operational modal filtration of synthesized FRFs

$$DI_{=}\frac{\int_{\omega_s}^{\omega_f}|x_i(\omega)-x_{\mathrm{ref}}(\omega)|^2\,\mathrm{d}\omega}{\int_{\omega_s}^{\omega_f}x_{\mathrm{ref}}(\omega)^2\mathrm{d}\omega} \tag{12}$$

where ω_s—starting frequency of the analyzed band, ω_f—closing frequency of the analyzed band, x_i—characteristic in the current state, x_{ref}—characteristic in the reference state.

To make the index sensitive mostly to structural changes, it is calculated only for the nearest (5 %) surrounding of the natural frequencies. In Table 3, the values of damage index are gathered together.

In the last step of operational modal filter verification, its application was compared with the modal filtration of the output PSDs as another method of damage detection from output-only data. To be precise, the scenarios no. 2 and 3 of the above list were proceeded and their results are placed in Fig. 8.

Also in this figure, on both plots, the area of natural frequency no. 5 is enlarged. It is clearly visible that filtration quality for the undamaged structure is much worse when the PSDs are filtered out. Also, the expected worsening of filtration quality for damage structure did not take place. The frequency of the peak was shifted of 2 Hz (due to drop of stiffness) but the magnitude of the not correctly filtered peak was smaller for the damaged case. This is caused by the fact that the excitation even in laboratory conditions was not so repeatable. Of course, for larger defects, the situation would likely go back to normal (worse results of modal filtering for the system with damage), but early fault detection is the primary goal of each algorithm of that kind.

5 Final conclusions

The paper presents an attempt to construct an application for modal filtration with the use of output-only data. The method is based on the replacement of originally measured FRFs (for which the excitation signal is required) with FRFs synthesized from the scaled operational modal model. The presented experimental verification showed that, with the use of in-operational data and only one impulse FRF, there is a possibility of a modal filter construction with comparable results to the classical one. Since the modal filter can be applied in many fields (see Sect. 1), thanks to the proposed innovation, all these applications will have a wider range. In the presented experimental verification, authors proved that the operational approach is suitable for the forces

Table 4 Pros and cons of different types of modal filtration of output only data

	OMF	CMF + PSDs
Output only data for the modal filter definition	+	−
Time of calculations	−	+
Possibility of automation	+/−	+
Accuracy of the calculations	+	−
Range of applications	+	−

identification. The comparison with the classical modal filter showed very small differences. Also, damage detection is possible with the use of operational modal filter with no worst quality than for modal filtration of the measured FRFs. Comparison with modal filtration of output-only data requires some discussion on con and pros. The quality of results in terms of early damage detection without risk of false alarms is of course the advantage of the proposed approach, also the modal filtration of PSDs is possible only for the objects excited with the white noise or similar signal that strongly limits the range of applications. On the other hand, by applying the operational modal filter, one loses the low computational cost and automation possibility. In Table 4, pros and cons analyses were placed.

The table shows that there are more advantages than drawbacks, and it is worth to use operational modal analysis for modal filter coefficient estimation.

References

1. Slater, G.L., Shelley, S.J.: Health monitoring of flexible structures using modal filter concepts. Proc. SPIE **1917**, 997–1008 (1993)
2. Gawronski, W., Sawicki, J.: Structural damage detection using modal norms. J. Sound Vib. **229**, 194–198 (2000)
3. El–Ouafi Bahlous, S., Abdelghani, M., Smaoui, H., El–Borgi, S.: Modal filtering and statistical approach to damage detection and diagnosis in structures using ambient vibrations measurements. J. Vib. Control **13**, 281–308 (2007)
4. Deraemaeker, A., Preumont, A.: Vibration based damage detection using large array sensors and spatial filters. Mech. Syst. Signal Process. **20**, 1615–1630 (2006)
5. Mendrok, K., Uhl, T.: The application of modal filters for damage detection. Smart Struct. Syst. **6**, 115–134 (2010)
6. Meirovitch, L., Baruh, H.: On the implementation of modal filters for control of structures. J. Guid. Control Dyn. **8**(6), 707–716 (1985)
7. Yeong-Ryeol, K., Kwang-Joon, K.: Indirect input identification by modal filter technique. Mech. Syst. Signal Process. **13**(6), 893–910 (1999)
8. Deshangere, G., Snoeys, R.: Indirect identification of excitation forces by modal coordinate transformation. In: Proc. of IMAC 3, pp. 685–690. Orlando, FL, February (1985)
9. Burgan, N.C., Snyder, S.D., Tanaka, N., Zander, A.C.: A generalized approach to modal filtering for active noise control—part I: vibration sensing. IEEE Sens. J. **2**(6), 577–589 (2002)
10. Hill, S.G., Snyder, S.D., Cazzolato, B.S., Tanaka, N., Fukuda, R.: A generalized approach to modal filtering for active noise control—part II: acoustic sensing. IEEE Sens. J. **2**(6), 590–596 (2002)
11. Spottswood, S.M., Allemang, R.J.: On the investigation of some parameter identification and experimental modal filtering issues for nonlinear reduced order models. Exp. Mech. **47**, 511–521 (2007)
12. Pagani, C.C. Jr., Trindade, M.A.: Optimization of modal filters based on arrays of piezoelectric sensors. Smart Mater. Struct. **18**(9), 095046 (2009)
13. Hwang, J., Kareem, A., Kim, W.: Estimation of modal loads using structural response. J. Sound Vib. **326**(3–5), 522–539 (2009)
14. Meirovitch, L., Baruh, H.: Control of self–adjoint distributed parameter system. J. Guid. Control Dyn. **8**, 60–66 (1982)
15. Zhang, Q., Shih, C.Y., Allemang, R.J.: Orthogonality Criterion for Experimental Modal Vectors: Vibration Analysis Techniques and Application, vol. 18–4, pp. 251–258. ASME publication, New York (1989)
16. Zhang, Q., Allemang, R.J., Brown, D.L.: Modal filter: concept and applications. In: Proceedings of 8th IMAC, pp. 487–496. Orlando, FL, USA (1990)
17. Schwarz, B., Richardson, M.: Using FEA modes to scale experimental mode shapes. In: Proceedings of 24th IMAC (2006)
18. Parloo, E., Verboven, P., Guillaume, P., Van Overmeire, M.: Sensitivity-based operational mode shape normalisation. Mech. Syst. Signal Process. **16**, 757–767 (2002)
19. Brincker, R., Andersen, P.: A way of getting scaled mode shapes in output only modal testing. In: Proceedings of the 21st IMAC. Kissimmee, FL (2003)
20. Parloo, E., Cauberghe, B., Benedettini, F., Alaggio, R., Guillaume, P.: Sensitivity-based operational mode shape normalisation: application to a bridge. Mech. Syst. Signal Process. **19**, 43–55 (2005)

21. Aenlle, M.L., Brincker, R., Canteli, A.F.: Some methods to determine scaled mode shapes in natural input modal analysis. In: Proceedings of the 23rd IMAC, Orlando, FL (2005)
22. Aenlle, M.L., Fernandez, P.F., Brincker, R., Canteli, A.F.: Scaling factor estimation using an optimized mass change strategy, part 1: theory. In: Proceedings of the 2nd International Operational Modal Analysis Conference, Copenhagen, Denmark (2007)
23. Foltête, E.: Multiple operational mode shapes normalisation from mass changes. In: Proceedings of the ISMA2008, Leuven, Belgium, pp. 2471–2480 (2008)
24. De Sitter, G., Parloo, E., Guillaume, P.: Operational vibro-acoustic modal analysis: mode shape normalisation. In: Proceedings of the XI Diname, Ouro Preto, Brazil (2005)
25. Deweer, J., Dierckx, B.: Obtaining a scaled modal model of panel type structures using acoustic excitation. In: Proceedings of the 17th IMAC, pp. 2042–2048 (1999)
26. Gao, Y., Randall, R.B.: Determination of frequency response functions from response measurements Part i: extraction of poles and zeros from response measurements. Mech. Syst. Signal Process. **10**, 293–317 (1996)
27. Gao, Y., Randall, R.B.: Determination of frequency response functions from response measurements Part ii: regeneration of frequency response functions from poles and zeros. Mech. Syst. Signal Process. **10**, 319–340 (1996)
28. Heylen, W., Lammens, S., Sas, P.: Modal Analysis Theory and Testing. Katholieke Universiteit Leuven, Departement Werktuigkunde, Leuven (1997)
29. Shih, C.Y., Zhang, Q., Allemang, R.J.: Force identification by using principle and modal coordinate transformation methods. In: Twelfth Biennial ASME Conference, Vibrational Analysis—Techniques and Applications, vol. 18–4, pp. 303–310. ASME, New York (1989)